

Effect of abrasive particle size on abrasive wear of hardfacing alloys

R. CHOTĚBORSKÝ¹, P. HRABĚ¹, M. MÜLLER¹, J. SAVKOVÁ², M. JIRKA¹,
M. NAVRÁTILOVÁ¹

¹*Department of Material Science and Manufacturing Technology, Faculty of Engineering,
Czech University of Life Sciences Prague, Prague, Czech Republic*

²*New Technologies Research Centre in Westbohemian Region – NTC,
University of West Bohemia, Pilsen, Czech Republic*

Abstract: Hardfacing is one of the most useful and economical ways to improve the performance of components submitted to severe wear conditions. This study has been made for the comparison of microstructure and abrasion resistance of hardfacing alloys reinforced with chromium carbides or complex carbides. The hardfacing alloys were deposited onto ČNS EN S235JR low carbon steel plates by the gas metal arc welding (GMAW) method. Different commercial hardfacing electrodes were applied to investigate the effect of abrasive particle size on abrasive wear resistance. The abrasion tests were made using the two-body abrasion test according to ČSN 01 5084 standard, abrasive cloths were of grits 80, 120, 240, and 400. Microstructure characterisation and surface analysis were made using optical and scanning electron microscopy. The results show the different influence of abrasive particles size on the wear rate for different structures of Fe-Cr-C system. The structures without primary carbides are of high abrasive wear rate, which increases nonlinearly with the increasing abrasive particle size. On the contrary, the structures containing primary carbides are of low abrasive rates and these rates increase linearly with the increasing abrasive particle size.

Keywords: hardfacing alloy; abrasive wear; pin-on-disk; carbide

Wear by hard particles occurs in many different situations such as with earth-moving equipment, slurry pumps or pipelines, rock drilling, rock or ore crushers, pneumatic transport of powders, dies in power metallurgy, extruders, or chutes. According to Figure 1, the wear processes may be classified by different modes depending on the kinematics and by mechanisms depending on the physical and chemical interactions between the elements of the tribosystem which result in detaching the material from the solid surfaces. Compared with the unlubricated sliding wear, the value of the wear coefficient k , i.e. the dimensionless quotient of the amount of volumetric wear W_v times the hardness of the wearing material H divided by the normal load F_N and the sliding distances, as estimated from practical experience, can be substantially greater in abrasive or erosive wear (ZUM GAHR 1998). Figure 1

can only represent a very rough estimation of the wear coefficient because of the wide variation of the wear mechanisms occurring in an actual tribosystem as a function of the operating conditions and properties of the triboelements involved, which can result in changes of the k value by some orders of magnitude.

In abrasive wear, the material is displaced or detached from the solid surface by hard particles or hard particles between or embedded in one or both of the two solid surfaces in relative motion, or by the presence of hard protuberances on the counterface sliding with the velocity v relatively along the surface. Two-body abrasion is caused by hard protuberances or embedded hard particles while in three-body abrasion the hard particles can move freely (roll or slide) between the contacting surfaces. According to SUCHÁNEK *et al.* (2007), the rate of the material

Supported by the Internal Grant Agency of the Czech University of Life Sciences in Prague, Faculty of Engineering, Project No. 31140/1312/313113.

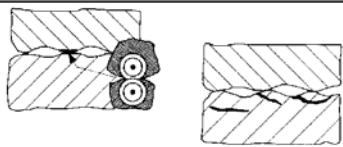



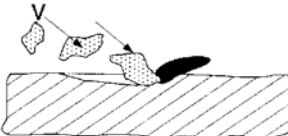
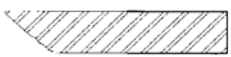
Wear mode	Wear mechanism	Wear coefficient $k = \frac{W_v \times H}{FN \times s}$
		10 ⁻⁷ 10 ⁻⁶ 10 ⁻⁵ 10 ⁻⁴ 10 ⁻³ 10 ⁻² 10 ⁻¹ 10 ⁰
Sliding wear		
Abrasive wear		
Erosive wear		

Figure 1. Values of wear coefficient k as a function of wear mechanism without lubricating media (ZUM GAHR 1998)

removal in three-body abrasion can be one order of magnitude lower than that for two-body abrasion, because the loose abrasive particles abrade the solid surfaces between which they are situated only about 10% of the time, while they spend about 90% of the time rolling. Hard particles striking a solid surface carried either by a gas or a liquid stream can cause erosive wear whereby the wear mechanism depends strongly on the angle of incidence of the impacting particles. The interaction between hard particles and the solid surface can be generally accompanied by the events of adhesion, abrasion, deformation, heating, surface fatigue, and fracture. Figure 2 shows schematically some general trends of the wear loss of

materials depending on the properties of the abrasive particles and the wearing materials as well as the operating conditions. With increasing hardness of the abrasive particles, the wear loss can increase by about one to two orders of magnitude from a low to a high level (Figure 2).

Models for two-body abrasion have been developed to a substantially greater depth than those for three-body abrasion. Penetration of a sliding abrasive particle into a metallic surface results in microploughing or microcutting depending on the attack angle. Below a critical attack angle, the metallic material is mainly elastically-plastically deformed and flows around and beneath the sliding

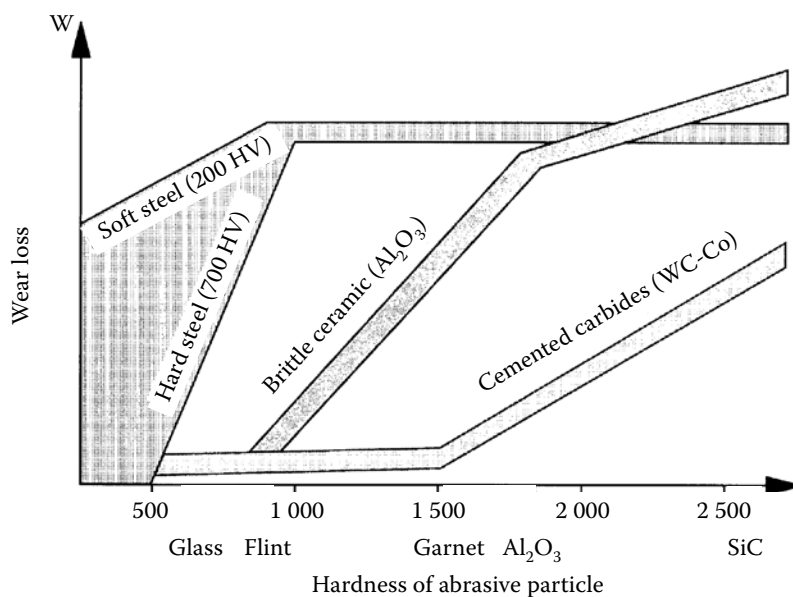


Figure 2. Schematic representation of wear loss by hard particles as a function of material properties such as hardness of abrasive particle (ZUM GAHR 1998)

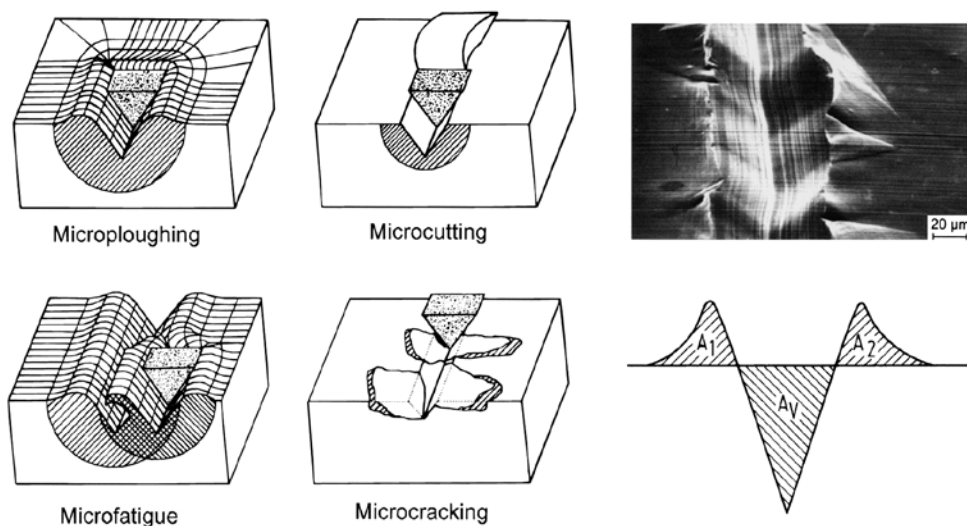


Figure 3. Schematic representation of different interactions between sliding abrasive particles and the surface of materials (ZUM GAHR 1998)

particle but no material is removed from the surface. Increasing the attack angle leads to a transition from microploughing to microcutting, i.e. material flows up the front face of the abrasive particle and is detached from the wearing surface in the form of a chip (ZUM GAHR 1998; COLACO & VILAR 2003a).

Hence, a more general model was developed which describes abrasive wear by distinguishing four types of interaction between the abrasive particles and wearing material (Figure 3), namely microploughing, microcutting, microfatigue, and microcracking. In the ideal case, microploughing, due to a single pass of one abrasive particle, does not result in any detachment of material from the wearing surface. A prow is formed ahead of the abrading particle and the material is continuously displaced sideways to form ridges adjacent to the groove produced. The volume loss can, however, occur owing to the action

of many abrasive particles or the repeated action of a single particle. The material may be ploughed aside repeatedly by passing particles and may break off by low cycle fatigue, i.e. microfatigue. Pure microcutting results in a volume loss by chips equal to the volume of the wear grooves. Microcracking occurs when highly concentrated stresses are imposed by abrasive particles, particularly on the surface of brittle materials. In this case, large wear debris is detached from the wearing surface owing to the crack formation and propagation. Microploughing and microcutting are the dominant processes on ductile materials while microcracking becomes important on brittle materials (ZUM GAHR 1998; SEVIM & ERYUREK 2006; SUCHÁNEK *et al.* 2007).

Composites can offer the answer for achieving high hardness and sufficient fracture toughness to avoid brittle fracture. Second phases, e.g. hard ce-

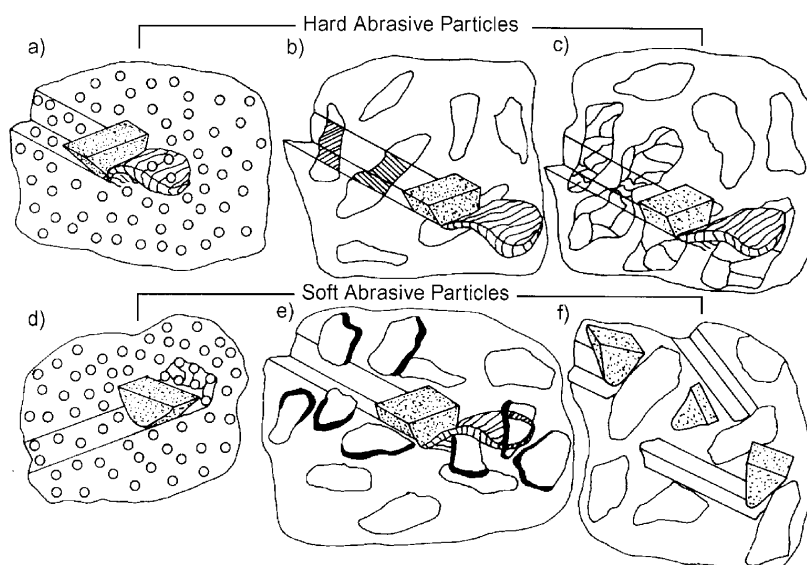


Figure 4. Interaction between sliding hard or soft abrasive particles and reinforcing phases (ZUM GAHR 1998)

ramic particles or fibers, can be incorporated into a softer and more ductile matrix. The abrasive wear resistance of such composites depends on different microstructural parameters such as the hardness, shape, size, volume fraction, and distribution of the embedded phases, the properties of the matrix and the interfacial bonding between the second phase and the matrix. Figure 4 shows different interactions between abrasive particles and a reinforcing phase. Hard and soft abrasive particles, i.e. harder or softer than the reinforcing phase, and also small and large sizes of the reinforcing phase are distinguished. Hard abrasive particles can easily dig out small phases and cut or crack larger ones. Soft abrasive particles are able to dig out small phases or produce large pits. The indentation depth of soft abrasive particles is substantially reduced by hard reinforcing phases if the mean free path between them is smaller than the size of the abrasive particles. Large phases deficiently bonded to the matrix can be pulled out. However, large phases strongly bonded to the matrix can blunt or fracture soft abrasive particles (COLACO & VILAR 2003b; BUCHELY *et al.* 2005).

Hardfacing made using flame, electric arc, or plasma, are used in industry. Hardfacing makes a strong metallurgical point between the deposit and substrate. Filler materials in the form of coated electrodes, cored electrodes, welding rods and powder represent a wide assortment of metal and composition materials of various properties. The choice of filler material and hardfacing technology depends on the part forms and dimensions, chemical composition of the substrate, mode of stress, wear type, and total cost for hardfacing. Tribological properties depend on the filler material chemical composition and on the hardfacing technology. In the first layer

of the deposit, the mixing of the filler material and substrate occurs. Therefore, the required properties are reached mostly in the second layer of multilayers (GÜLENC & KAHRAMAN 2003; YILMAZ 2006; CORREA *et al.* 2007a,b).

Hardfacing materials of major volume of carbidic phase in the deposit are of a very good abrasion resistance. For usual temperatures, hardfacing materials on the basis of Fe-Cr-C are used, above all for their relatively low price. Complex deposit Fe-Cr-C-M (where M means Nb, W, Ti, Mo and their combination) are of higher abrasion resistance. The commercially produced hardfacing materials are usually of 3–5.5% carbon content (ATAMERT & BHADESHIA 1990; ASENSIO *et al.* 2003). By the use of these electrodes on the low carbon steel as substrate and one layer deposit, the hypoeutectic or eutectic structure is reached. In the case of complex alloyed deposit, the hypoeutectic structure with primary carbides of MC type (e.g. NbC, WC) occurs. The carbides M_7C_3 with high Cr contents can be reached only in the second and next layers (PING LU *et al.* 2004; CHOTĚBORSKÝ 2008; JANKAUSKAS *et al.* 2008).

EXPERIMENTAL PROCEDURE

Materials and welding conditions

Steel according to ČSN EN S235JR was used as the substrate. Its composition, determined using the GDOES method, is presented in Table 1. The substrate plate used for surfacing was of dimensions 100 × 25 × 300 mm.

On this substrate plate, the filler materials were deposited. Their nominal chemical composition is presented in Table 2, welding conditions in Table 3.

Hardness measurement

The bulk hardness of the hardfacing deposits was measured by the Vickers hardness method, while a

Table 1. Chemical composition of substrate plate (weight %)

C	Mn	S	P	Fe
0.074	0.33	0.006	0.0025	balance

Table 2. Chemical composition of electrodes (weight %)

	C	Cr	Nb	Mo	W	V	Si	Mn	Fe
Hardfacing 1 (H1)	3.2	29	–	–	–	–	1.0	–	balance
Hardfacing 2 (H2)	3.5	35	–	–	–	–	1.0	–	balance
Hardfacing 3 (H3)	4.4	23.5	5.5	6.5	2.2	1.5	–	–	balance
Hardfacing 4 (H4)	3.8	33	–	0.5	–	–	1.2	–	balance
Hardfacing 5 (H5)	4.5	17.5	5	1.0	1.0	1.0	0.5	0.5	balance
Hardfacing 6 (H6)	3.5	22	–	3.5	–	0.4	0.4	0.9	balance

Table 3. Welding conditions

Electrode diameter (mm)	1.6
Arc voltage (V)	27
Welding current (A)	250
Electrode polarity	positive
Welding speed (cm/min)	13
Preheating	no
Deposition rate (kg/h)	14.3

microhardness tester allowed measuring the hardness of the phases in the microstructure by using a Vickers indenter with a load of 0.1 kg.

Microstructure analysis

Optical and scanning electron microscopes were used to analyse the microstructure of the specimens. Secondary electron imaging allowed morphologic description of the worn surfaces, while backscattered electron imaging and EDX compositional were used to describe qualitatively the chemical composition of the phases in the microstructure.

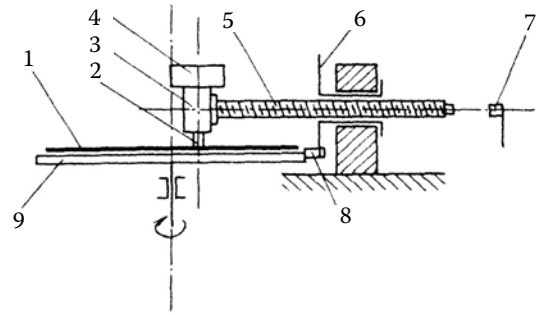


Figure 5. Diagrammatic representation of the pin-on-disk testing machine: 1 – abrasive cloth, 2 – specimen, 3 – holder, 4 – weight, 5 – screw, 6 – nut with cogs, 7 – limit switch, 8 – pin, 9 – horizontal plate

Abrasive wear

The abrasive wear resistance was tested using the tester with bonded abrasive according to ČSN 01 5084 (1974). For the test, the abrasive cloth of 80, 120, 240, and 400 grits and the load of 2.35 kg were chosen. The mass lost was determined using the analytic balance of 0.0001 accuracy. The pin-on-disk testing machine (Figure 5) consists of a uniformly rotating disk whereon the abrasive cloth is fixed. The tested specimen is fixed in the holder and pressed

Table 4. Chemical composition of weld deposit layers (weight %)

	C	Cr	Nb	Mo	W	V	Si	Mn	Fe
First layer									
Hardfacing 1 (H1)	2.93	26.31	–	0.6	–	0.19	1.06	1.0	balance
Hardfacing 2 (H2)	2.04	30.3	–	–	–	0.1	0.76	0.13	balance
Hardfacing 3 (H3)	4.27	19.1	4.64	4.44	0.75	1.35	1.08	0.21	balance
Hardfacing 4 (H4)	2.28	20.86	–	0.27	–	0.1	0.45	0.1	balance
Hardfacing 5 (H5)	3.5	12.42	2.45	0.59	0.31	0.63	0.38	0.55	balance
Hardfacing 6 (H6)	3.7	17.21	–	2.7	–	0.5	0.34	0.85	balance
Second layer									
Hardfacing 1 (H1)	3.03	32.27	–	0.64	–	0.20	1.07	1.03	balance
Hardfacing 2 (H2)	2.93	31.16	–	–	–	0.18	0.80	0.15	balance
Hardfacing 3 (H3)	4.43	21.51	5.26	4.65	0.95	1.52	1.13	0.24	balance
Hardfacing 4 (H4)	3.03	31.98	–	0.36	–	0.15	0.64	0.15	balance
Hardfacing 5 (H5)	5.01	16.79	7.74	0.67	0.53	0.81	0.49	0.49	balance
Hardfacing 6 (H6)	3.9	18.65	–	2.9	–	0.55	0.33	0.84	balance
Third layer									
Hardfacing 1 (H1)	3.1	33.36	–	0.66	–	0.20	1.17	1.07	balance
Hardfacing 2 (H2)	2.94	32.83	–	–	–	0.20	0.88	0.21	balance
Hardfacing 4 (H4)	3.41	32.78	–	0.42	–	0.17	0.68	0.17	balance

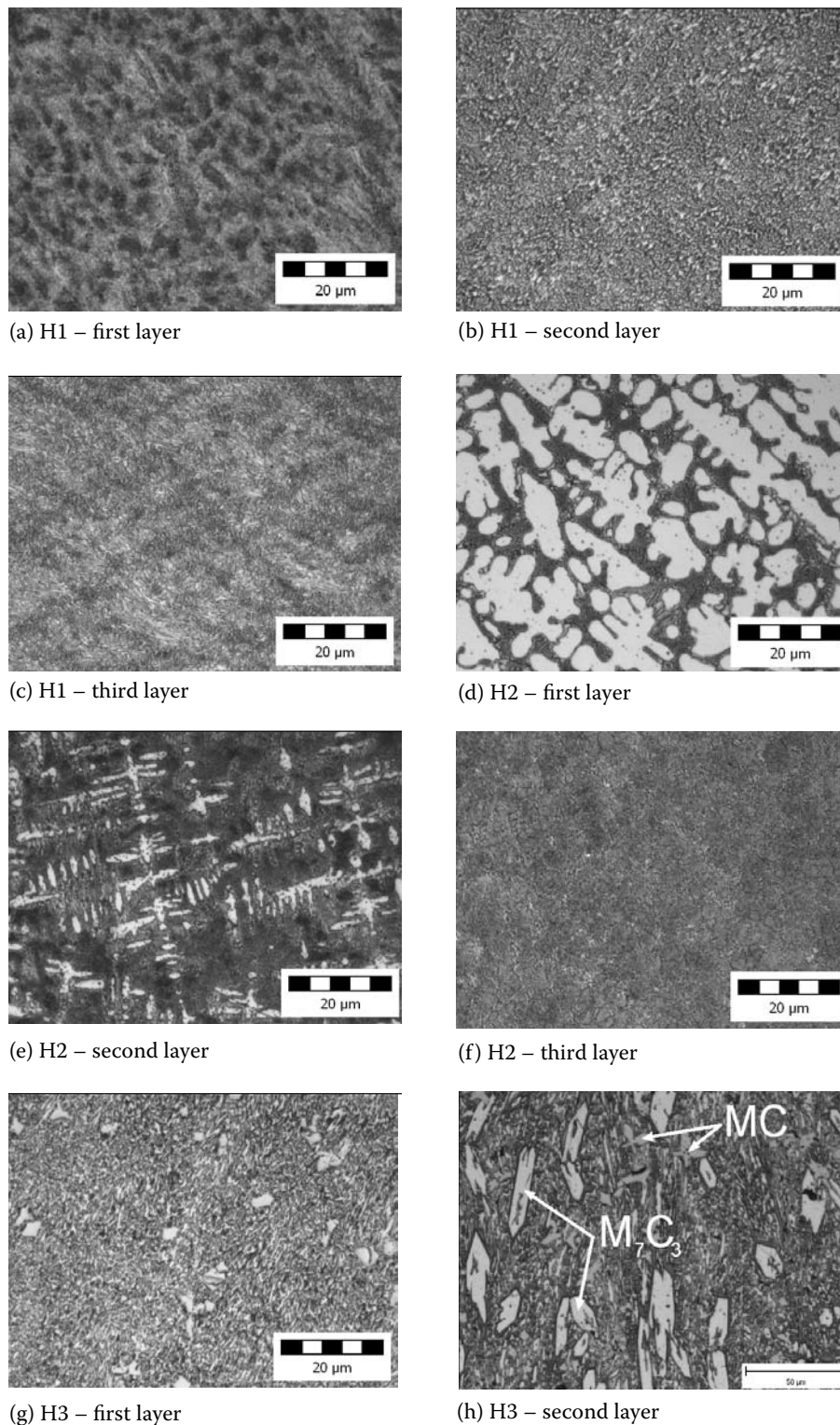


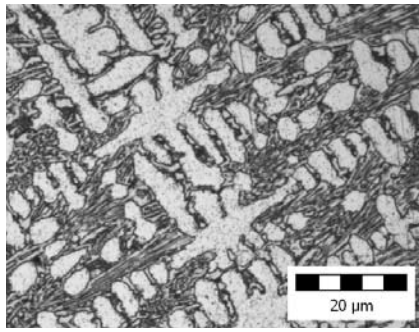
Figure 6. Structures of deposit using the optical microscopy

against the abrasive cloth by the weight of 2.35 kg. A screw makes possible the radial feed of the specimen. The limit switch stops the test. During the test the specimen moves from the outer edge to the centre of the abrasive cloth and a part of the specimen comes in contact with the unused abrasive cloth.

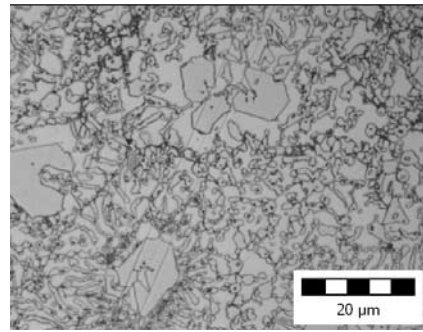
RESULTS AND DISCUSSION

Chemical composition and microstructure

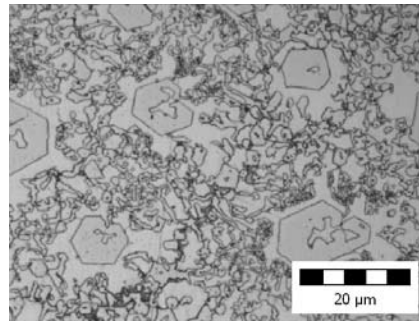
Table 4 presents the chemical compositions of the weld deposit layers. It is evident that the chemical



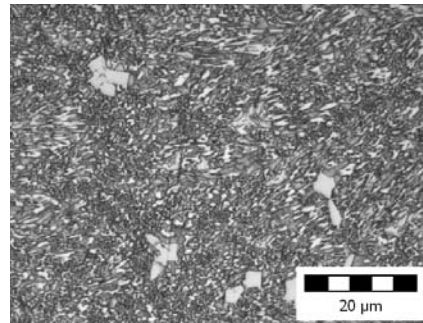
(i) H4 – first layer



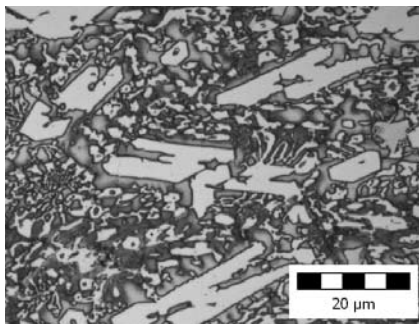
(j) H4 – second layer



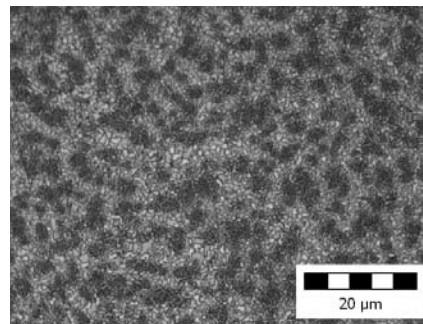
(k) H4 – third layer



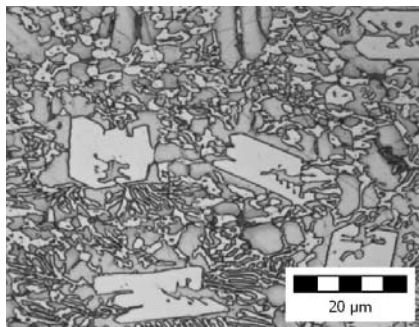
(l) H5 – first layer



(m) H5 – second layer



(n) H6 – first layer

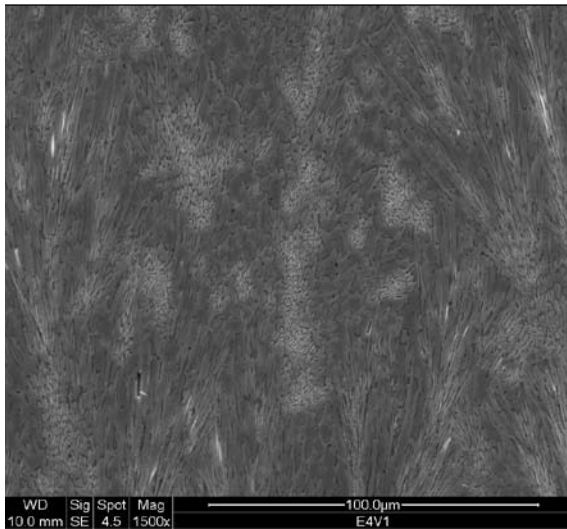


(o) H6 – first layer

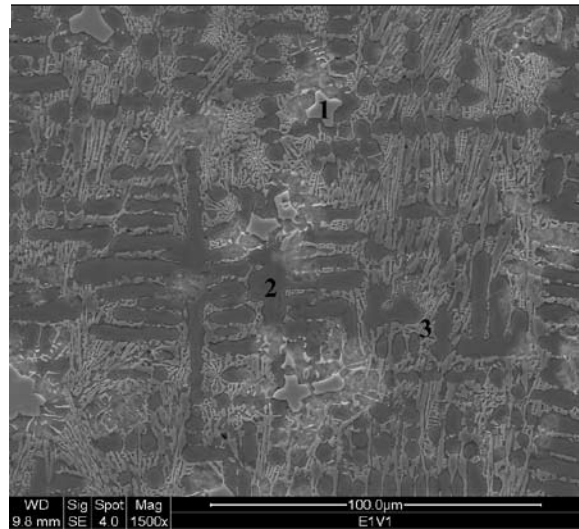
Figure 6. continued

composition approximately equal to the filler wire composition is reached in the second and further layers. The difference between the second and third layers is not so much expressive and the layers structures are the same. The lower content of carbon and alloying elements in the first layer is caused by mix-

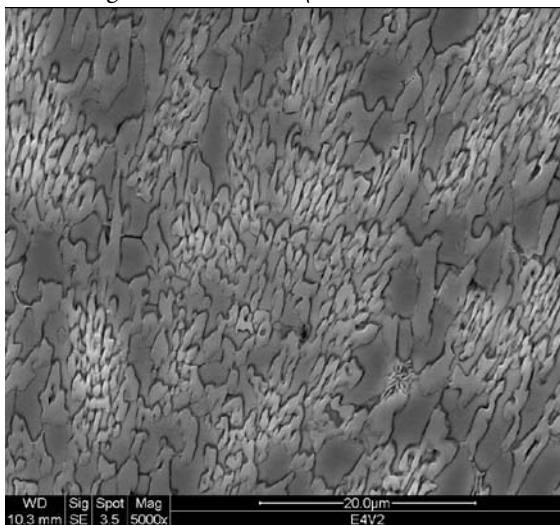
ing the overlay and low carbon substrate materials. This problem can be solved e.g. by the use of powder graphite and alloys added in the course of hardfacing. This method was successfully used e.g. by WANG *et al.* 2006, when the powder graphite was added in the welding flux. E.g. WANG tested the alloying using



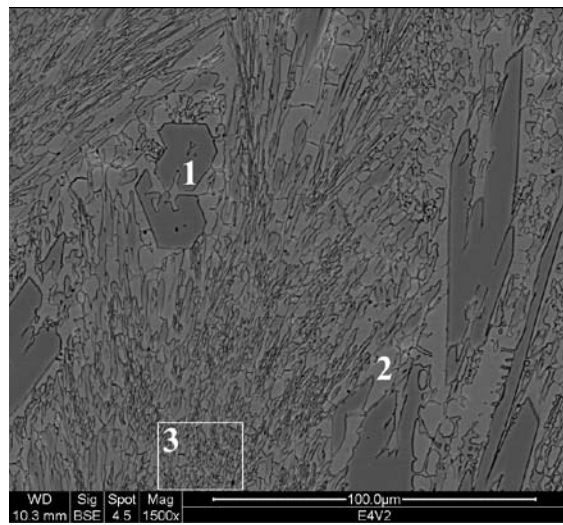
(a) E4V1, WD-10.0 mm, Sig-SE, Spot -4.5, Mag-1 500 x, 1 000.0 μm



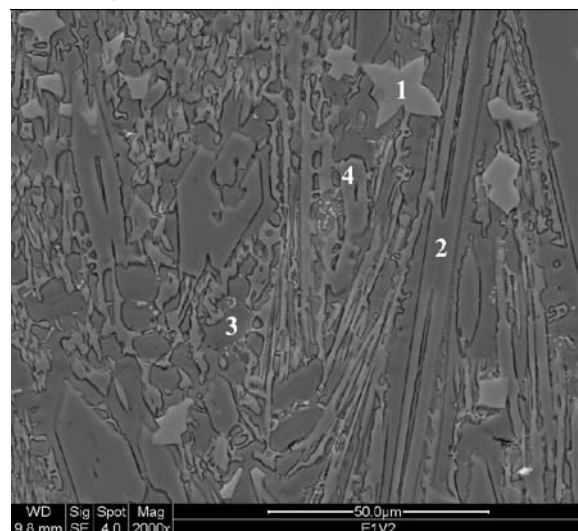
(b) E1V1, WD-9.8 mm, Sig-SE, Spot -4.0, Mag-1 500 x, 100.0 μm



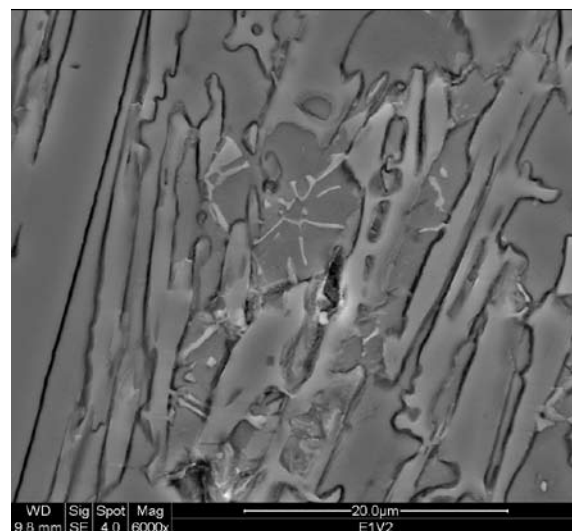
(c) E4V2, WD-10.3 mm, Sig-SE, Spot -3.5, Mag-5 000 x, 20.0 μm



(d) E4V2, WD-10.3 mm, Sig-BSE, Spot -4.5, Mag-1 500 x, 100.0 μm



(e) E1V2, WD-9.8 mm, Sig-SE, Spot -4.0, Mag-2 000 x, 50.0 μm



(f) E1V2, WD-9.8 mm, Sig-SE, Spot -4.0, Mag-6 000 x, 20.0 μm

Figure 7. Structures of the some deposit using SEM

Table 5. Hardness of hardfacing layers (HV30)

	Hardfacing 1	Hardfacing 2	Hardfacing 3	Hardfacing 4	Hardfacing 5	Hardfacing 6
First layer	617	492	714	465	612	606
Second layer	680	564	812	560	778	646
Third layer	696	638	–	595	–	–

powder of high carbon ferrochromium mixed with welding flux for SAW surfacing method. The results can be found e.g. in works of WANG (WANG *et al.* 2007, 2008a,b,c).

Figure 6 shows the deposit structures corresponding to the chemical compositions presented in Table 4. The structures of one layer deposits (H1, H2, H4, H6) are created by carbidic eutectic and austenite. The morphology of carbidic eutectic consisting of carbide (Fe, Cr)₇C₃ and austenite is showed in Figure 7a. The deposits without primary carbides contain this type of carbidic eutectic. The structures of complex alloyed deposit materials (H3, H5) are created by carbidic eutectic on the basis of M₇C₃, austenite, and primary carbides of MC type (Figure 7b for H5).

The structure of two layers deposit is created by primary carbides, carbidic eutectic (Figure 7c), and austenite. The primary carbides of M₇C₃ (Figure 7d) are in the weld deposits of H1, H2, H4, and H6. The neighbourhood of these carbides is austenitic. The second layer of the complex alloyed deposit is created by primary carbides MC a M₇C₃, carbidic

eutectic, and austenite (Figure 7e). The eutectic morphology is shown in Figure 7f.

Hardness

The Vickers hardness (HV) values are presented in Table 5 for one-layer, two-layer, and three-layer deposits. The hardness of the deposit corresponds to the structure. The lowest hardness values were determined in one-layer deposit materials alloyed only with chromium. The hardness of these deposits is influenced by the proportion of phases. The deposit containing the highest amount of austenite is of the lowest hardness. The hardness increases with the carbidic eutectic quantity. The complex alloyed deposits in the second or third layers with primary carbides contents are of the highest hardness values. The hardness values of these deposits increase with the carbidic phase amount and size. Except the deposit bulk hardness, the hardness of single phases is also determined (if the phase size is sufficient for HV_{0.01} measuring). Table 6 shows the hardness of single microstructure phases of deposits.

Table 6. Hardness of phases in the hardfacing

Phase	Austenite (HV _{0.02})	Eutectic (HV _{0.02})	MC (HV _{0.1})	M ₇ C ₃ (HV _{0.1})
H2 first layer	650	930	–	–
H2 second layer	612	950	–	–
H2 third layer	–	965	–	–
H3 first layer	700	1 130	1 850	–
H3 second layer	730	1 150	1 850	1 600
H4 first layer	642	940	–	–
H4 second layer	635	1 050	–	1 550
H4 third layer	640	1 020	–	1 560
H5 first layer	–	1 120	1 800	–
H5 second layer	720	1 150	1 800	1 635
H6 first layer	–	873	–	–
H6 second layer	650	870	–	1 600

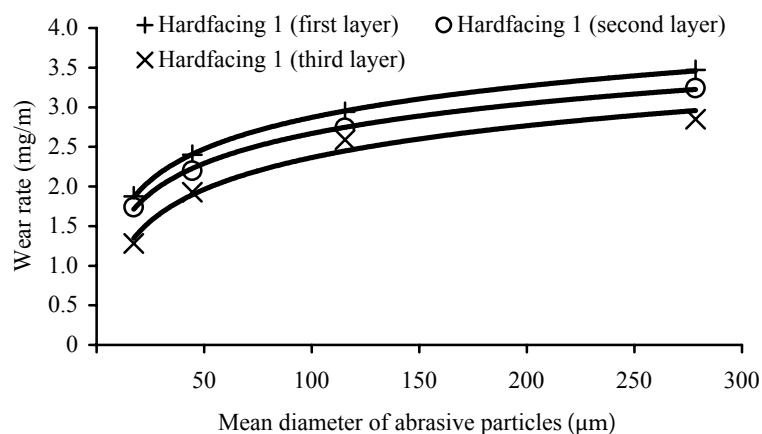


Figure 8. Hardfacing 1 – relation between wear rate and abrasive particles size

Abrasive wear and roughness

Figures 8–13 show the abrasive wear resistance results of the hardfacings tested. From the results it follows that the structure is of a significant influ-

ence on the wear resistance. With the hardfacing of eutectic or hypoeutectic structures, the dependence between the wear rate and abrasive particles mean diameter is linear. The wear rate of these hardfacings depends significantly on the proportions of carbidic

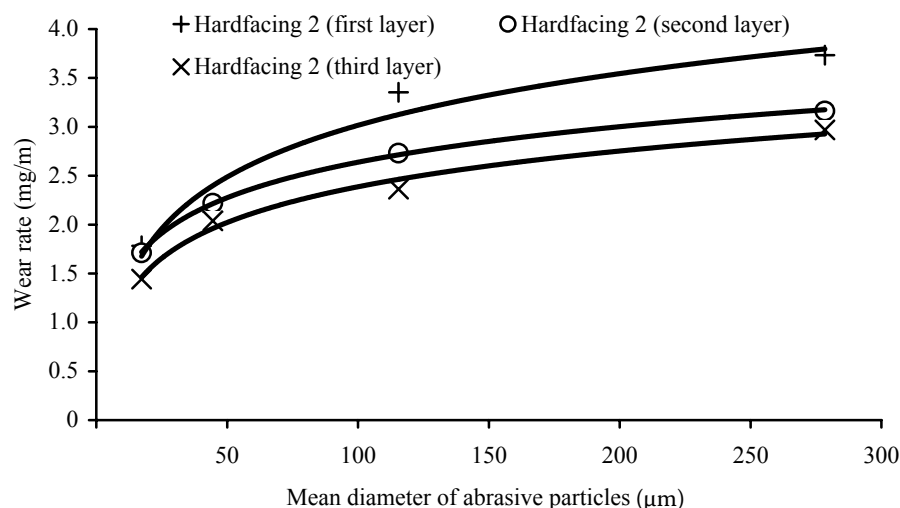


Figure 9. Hardfacing 2 – relation between wear rate and abrasive particles size

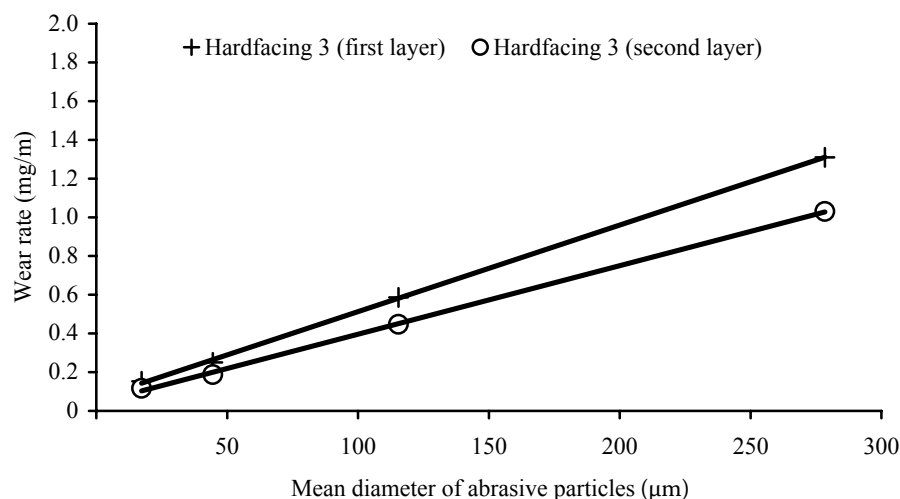


Figure 10. Hardfacing 3 – relation between wear rate and abrasive particles size

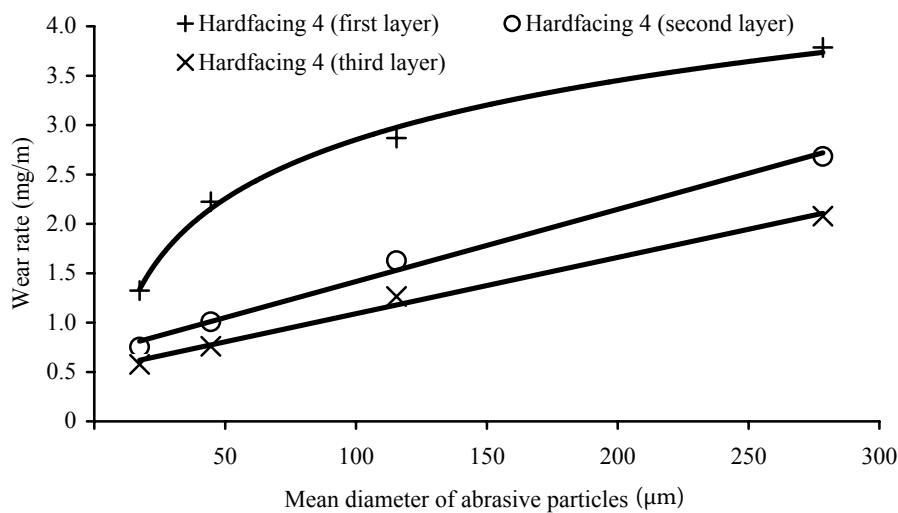


Figure 11. Hardfacing 4 – relation between wear rate and abrasive particles size

eutectic and austenite. The higher the carbidic eutectic content in the hardfacing structure, the lower the wear rate.

With the occurrence of primary carbides in the structure, the wear rate increases linearly with the

abrasive particle size. The wear rate decreases with the carbidic phase amount. In the first layer, the hardfacing 3 contains a higher quantity of primary carbides MC than the hardfacing 5 and the carbidic eutectic and austenite matrix shows a higher repre-

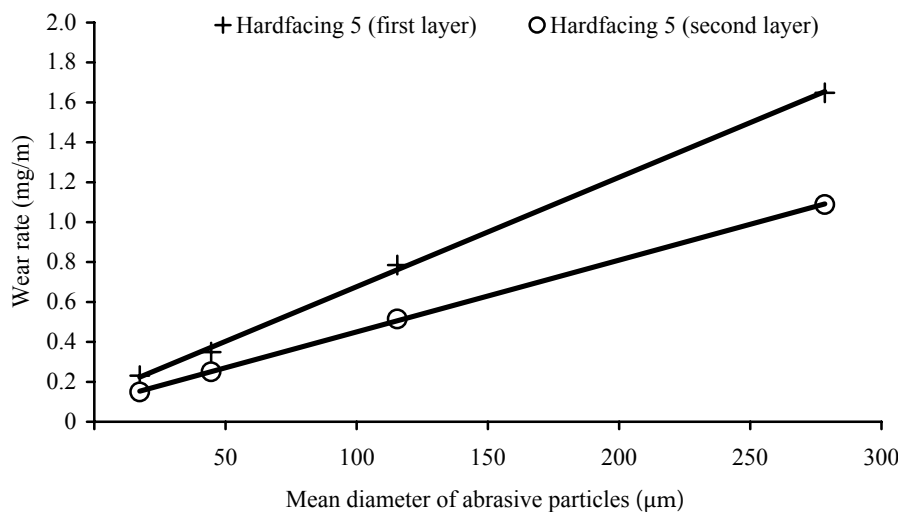


Figure 12. Hardfacing 5 – relation between wear rate and abrasive particles size

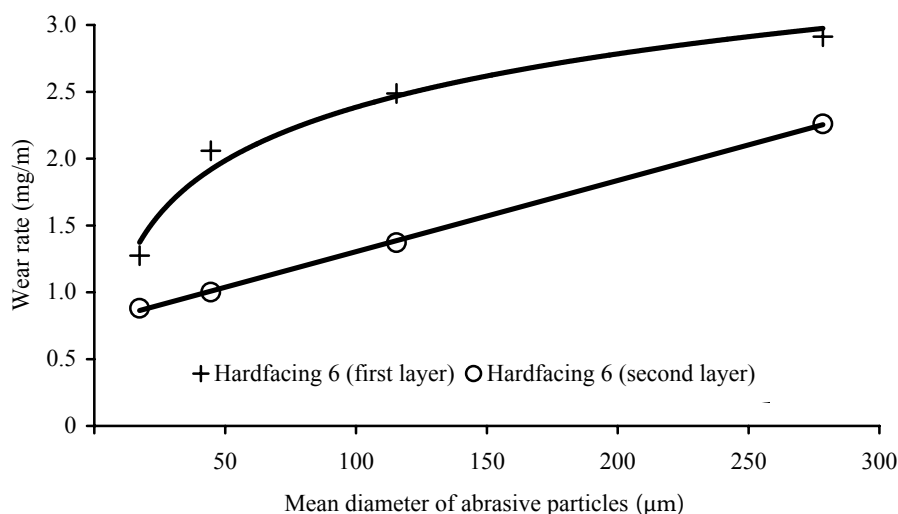


Figure 13. Hardfacing 6 – relation between wear rate and abrasive particles size

sentation of austenite. The works of SUCHÁNEK present that this austenite, if deformed, transforms into martensite. In the second layer of hardfacings 3 and 5, the carbides MC and M_7C_3 occur. The quantities of M_7C_3 and its sizes is almost identical and therefore the wear rate is of the same value. A slightly lower wear rate is found in the hardfacing 3, evidently because of the higher content of MC phase.

E.g. in the first layer of hardfacings 4 and 6 no primary carbides occur and the structure consists of carbidic eutectic and austenite. In the third layer of hardfacing 4 and in the second layer of hardfacing 6 primary carbides M_7C_3 already occur and the wear rate decreases significantly. The character of the wear rate dependence on the abrasive particles size changes to linear.

CONCLUSION

The knowledge obtained can be summarised in the following points:

The hardness of hypoeutectic hardfacings increases with the carbidic eutectic part and type. The hardness of hypereutectic hardfacing increases with the increasing proportions of carbidic phases MC and M_7C_3 .

The abrasive wear rate of hypoeutectic hardfacing depends on the structural components portions. A higher part of alloyed eutectic reduces the wear rate.

The dependence of hypoeutectic deposit abrasive wear rate on the abrasive particles size is not linear. This fact can be caused by the abrasive particle critical size, which erodes the carbidic eutectic softer phase and in this way uncovers the carbidic phase which can crumble away. This dependence of the abrasive wear rate increase on the increase of the abrasive particle size is almost constant.

The abrasive wear rate of hypereutectic hardfacing decreases with the increasing proportions of carbidic phases MC and M_7C_3 . In this decrease, the MC phase participates more because it is harder. This is shown in comparing the hardfacings 3, 4, 5, and 6.

The dependence between the hypereutectic hardfacings wear rate and the abrasive particle size is linear.

References

- ASENSIO J., PERO-SANZ J.A., VERDEJA J. I. (2003): Microstructure selection criteria for cast irons with more than 10 wt.% chromium for wear applications. *Materials Characterization*, **49**: 83–93.
- ATAMERT S., BHADESHIA H.K.D.H. (1990): Microstructure and stability of Fe-Cr-C hardfacing alloys. *Materials Science and Engineering A*, **130**: 101–111.
- BUCHELY M.F., GUTIERREZ J.C., LEÓN L.M., TORO A. (2005): The effect of microstructure on abrasive wear of hardfacing alloys. *Wear*, **259**: 52–61.
- CHOTĚBORSKÝ R., HRABĚ P., MÜLLER M., SAVKOVÁ J., JIRKA M. (2008): Abrasive wear of high chromium Fe-Cr-C hardfacing alloys. *Research Agriculture Engineering*, **54**: 192–198.
- COLACO R., VILAR R.A. (2003a): Model for the abrasive wear of metallic matrix particle-reinforced materials. *Wear*, **254**: 625–634.
- COLACO R., VILAR R.A. (2003b): Abrasive wear of metallix matrix reinforced materials. *Wear*, **255**: 643–650.
- CORREA E.O., ALCANTARA N.G., TECCO D.G., KUMAR R.V. (2007a): Development of an iron-based hardfacing material reinforced with Fe-(TiW)C composite powder. *Metallurgical and Materials Transactions A*, **38**: 937–945.
- CORREA E.O., ALCÂNTARA, N.G., TECCO, D.G., KUMAR, R.V. (2007b): The relationship between the microstructure and abrasive resistance of a hardfacing alloy in the Fe-Cr-C-Nb-V system. *Metallurgical and Materials Transaction A*, **38**: 1671–1680.
- GÜLENC B., KAHRAMAN N. (2003): Wear behaviour of bulldozer rollers welded using a submerged arc welding process. *Materials and Design*, **24**: 537–542.
- JANKAUSKAS V., KREIVAITIS R., MILČIUS D., BALTUŠNIKAS A. (2008): Analysis of abrasive wear performance of arc welded hard layers. *Wear*, doi:10.1016/j.wear.2008.03.022.
- PING LU SHAN, OH-YANG KWON, TAE-BUM KIM, KWON-HU KIM (2004): Microstructure and wear property of Fe-Mn-Cr-Mo-V alloy cladding by submerged arc welding. *Journal of Material Processing Technology*, **147**: 191–196.
- SEVIM I., ERYUREK B.I. (2006): Effect of abrasive particle size on wear resistance in steels. *Materials and Design*, **27**: 173–181.
- SUCHÁNEK J., KUKLÍK V., ZDRAVECKÁ E. (2007): Abrasive wear of materials. CTU Prague, Praha, 162. (in Czech)
- WANG X.H., SONG S.L., ZOU Z.D., QU S.Y. (2006): Fabricating TiC particles reinforced Fe-based composite coatings produced by GTAW multi-layers melting process. *Materials Science and Engineering A*, **441**: 60–67.
- WANG X.H., SONG S.L., QU S.Y., ZOU Z.D. (2007): Characterization of in situ synthesized TiC particle reinforced Fe-based composite coatings produced by multi-pass overlapping GTAW melting process. *Surface and Coatings Technology*, **201**: 5899–5905.
- WANG X.H., HAN F., QU S.Y., ZOU Z.D. (2008a): Microstructure of the Fe-based hardfacing layers reinforced by TiC-VC-Mo₂C particles. *Surface and Coatings Technology*, **202**: 1502–1509.
- WANG X.H., HAN F., LIU X.M., QU S.Y., ZOU Z.D. (2008b): Microstructure and wear properties of the Fe-Ti-V-Mo-C hardfacing alloy. *Wear*, **256**: 583–589.
- WANG X.H., HAN F., LIU X.M., QU S.Y., ZOU Z.D. (2008c): Effect of molybdenum on the microstructure and wear

- resistance of Fe-based hardfacing coatings. *Materials Science and Engineering A*, **489**: 193–200.
- YILMAZ S.O. (2006): Wear behavior of gas tungsten arc deposited FeCr, FeCrC, and WC coatings on AISI 1018 steel. *Surface and Coatings Technology*, **201**: 1568–1575.
- ZUM GAHR K.H. (1998): Wear by hard particles. *Tribology International*, **31**: 587–596.
- Received for publication October 10, 2008
Accepted after corrections May 6, 2009

Abstrakt

CHOTĚBORSKÝ R., HRABĚ P., MÜLLER M., SAVKOVÁ J., JIRKA M., NAVRÁTILOVÁ M. (2008): **Vliv velikosti abrazivní částice na abrazivní opotřebení návarových materiálů.** *Res. Agr. Eng.*, **55**: 101–113.

Návarové vrstvy jsou jednou z cest ke zvýšení odolnosti proti opotřebení a zároveň jsou i ekonomickou cestou. Studie porovnává mikrostrukturní charakteristiky návarových materiálů a odolnost vůči abrazivnímu opotřebení. Studium bylo prováděno na návarových materiálech, kde ve struktuře byly chromové karbidy a karbidy komplexní. Návarový materiál byl nanesen na nízkouhlikovou ocel S235JR metodou odtavující se elektrody v ochranné atmosféře. Různé komerční návarové materiály byly studovány z hlediska efektu velikosti abrazivní částice na abrazivní opotřebení. Test abrazivního opotřebení byl prováděn na brusném plátně o zrnitosti 80, 120, 240 a 400 podle ČSN 01 5084. Charakteristika mikrostruktury a analýza povrchu byla prováděna postupy optické a elektronové mikroskopie. Výsledky ukazují rozdílný vliv velikosti abrazivní částice na rychlost opotřebení pro různé struktury systému Fe-Cr-C. Struktury bez primárních karbidů mají vysokou rychlost abrazivního opotřebení; tato rychlost roste nelineárně se zvětšující se velikostí abrazivní částice. Naopak struktury s primárními karbidy mají nízkou rychlost abrazivního opotřebení a tato rychlost roste lineárně se zvětšující se abrazivní částicí.

Klíčová slova: návarový materiál; abrazivní opotřebení; pin-on-disk; karbidy

Corresponding author:

Ing. ROSTISLAV CHOTĚBORSKÝ, Ph.D., Česká zemědělská univerzita v Praze, Technická fakulta, katedra materiálu a strojírenské technologie, Kamýcká 129, 165 21 Praha 6-Suchbát, Česká Republika
tel.: + 420 224 383 274, fax: + 420 234 381 828, e-mail: choteborsky@tf.czu.cz
